

Dynamics of Nucleosomes Revealed by Time-Lapse Atomic Force Microscopy[†]

Luda S. Shlyakhtenko, Alexander Y. Lushnikov, and Yuri L. Lyubchenko*

Department of Pharmaceutical Sciences, College of Pharmacy, University of Nebraska Medical Center, Omaha, Nebraska 68198-6025

Received June 11, 2009; Revised Manuscript Received July 10, 2009

ABSTRACT: The dynamics of chromatin provides the access to DNA within nucleosomes, and therefore, this process is critically involved in the regulation of chromatin function. However, our knowledge of the large-range dynamics of nucleosomes is limited. Answers to the questions, such as the range of opening of the nucleosome and the mechanism via which the opening occurs and propagates, remain unknown. Here we applied single-molecule time-lapse atomic force microscopy (AFM) imaging to directly visualize the dynamics of nucleosomes and identify the mechanism of the large range DNA exposure. With this technique, we are able to observe the process of unwrapping of nucleosomes. The unwrapping of nucleosomes proceeds from the ends of the particles, allowing for the unwrapping of DNA regions as large as dozens of base pairs. This process may lead to a complete unfolding of nucleosomes and dissociation of the histone core from the complex. The unwrapping occurs in the absence of proteins involved in the chromatin remodeling that require ATP hydrolysis for their function, suggesting that the inherent dynamics of nucleosomes can contribute to the chromatin unwrapping process. These findings shed a new light on molecular mechanisms of nucleosome dynamics and provide novel hypotheses about the understanding of the action of remodeling proteins as well as other intracellular systems in chromatin dynamics.

The dynamics of the nucleosome core particle (NCP),¹ a fundamental unit of chromatin, is a key property of chromatin, providing access to the DNA wrapped around the histone core of the protein. These NCP dynamics are also important in accomplishing the other numerous functions of chromatin. Studies performed over the past decade led to the discovery of a class of proteins, the exclusive role of which is to regulate the DNA accessibility within the chromatin (e.g., reviews (1–3)). These specialized remodeling machines unwrap the DNA from the histone core to provide the access to the DNA regions inside the nucleosome. This discovery led to the view in which nucleosomes themselves are considered rather stable particles with limited dynamics, so the nucleosome unwrapping process is performed by remodeling protein complexes in an ATP-dependent fashion (3, 4). The reconciliation of this model with the energetic costs required for the unwrapping of DNA from the nucleosome core particle led to the model in which remodeling proteins use the ATP hydrolysis energy to unwrap only a segment of the nucleosomal DNA, creating a bulge and then moving that bulge along the histone like a ratchet (3). At the same time, recent studies performed with the use of various techniques, including single-molecule approaches, led to the realization that nucleosomes are quite dynamic rather than static systems. Therefore, the inherent dynamics should be taken into account in attempting to understand the nucleosome unwrapping process. Single-molecule fluorescence and time-resolved techniques showed that nucleosomes undergo local dissociation of DNA in the absence of

remodeling proteins (5–11), and this process occurs on the subsecond time scale (8, 10). Previously, AFM imaging was applied to the characterization of chromatin structure at the nanoscale level (12–15). The AFM sample preparation is so gentle that AFM enables the study of chromatin structure omitting the rather traditional glutaraldehyde fixation procedure of the sample (16). As a result, the comparison of fixed and unfixed samples led the authors to the conclusion about the high dynamic feature of nucleosomes. However, a number of questions remained unanswered. What is the range of the local dynamics of nucleosomes? Is a non-ATP-dependent unwrapping of nucleosomes possible? What are the factors facilitating the large-scale opening and unwrapping of nucleosomes? To answer these questions, we used a single-molecule time-lapse AFM approach capable of detecting the dynamics of molecular systems at the single-molecule level (17–19). Previously, this capability of time-lapse AFM enabled us to follow the dynamics of supercoiled DNA (20), including the dynamics of cruciform structures (21), and to directly test the models of the Holliday junction branch migration (22, 23). The development of high-speed AFM, with the ability to perform time-lapse AFM imaging at speeds much faster than those of traditional AFM techniques, is also notable (24, 25). Given the capability of time-lapse AFM to image the dynamics of molecular systems at nanoscale, we applied this method to study the dynamics of mononucleosome samples. We were able to directly visualize large-scale dynamics of nucleosomes, accompanied with unwrapping of long DNA regions, followed by the complete unwrapping of DNA from the histone core, and the dissociation of nucleosome particles. The possibility of unwrapping nucleosomes in the absence of the ATP-dependent chromatin remodeling proteins under low-salt conditions is a feature of nucleosomes, dramatically facilitating the DNA accessibility problem and prompting new models of the regulation of the nucleosome unwrapping process.

[†]This work is supported by Grants EPS-0701892 and PHY-0615590 (both from the National Science Foundation) and Grant GM062235 (from the National Institutes of Health) to Y.L.L.

*To whom correspondence should be addressed: Department of Pharmaceutical Sciences, University of Nebraska Medical Center, 986025 Nebraska Medical Center, Omaha, NE 68198-6025. Phone: (402) 559-1971. Fax: (402) 559-9543. E-mail: ylyubchenko@unmc.edu.

Abbreviations: AFM, atomic force microscopy; NCP, nucleosome core particle; APS, 1-(3-aminopropyl)silatrane.

MATERIALS AND METHODS

Reconstitution of the Histone Octamer. Reconstitution of NCP was performed according to the procedure described in refs 26 and 27. Briefly, the human recombinant histones H2A, H2B, H3, and H4 (New England Biolab, Ipswich, MA) were concentrated on a Microcon spin column (MW 3000, Millipore, Billerica, MA) and dissolved in unfolding buffer (UB) containing 6 M guanidine chloride, 20 mM Tris-HCl (pH 7.5), and 5 mM DTT. The concentration of each histone protein was measured by the absorbance spectra at 276 nm. After incubation for 1 h at room temperature, all four histone proteins were mixed in an equimolar ratio and diluted up to 1 mg/mL with refolding buffer (RB), containing 2 M NaCl, 10 mM Tris-HCl (pH 7.5), 1 mM EDTA, and 5 mM 2-mercaptoethanol. After the precipitated protein had been removed by centrifugation for 10 min at 12700g, the sample were loaded on a Superdex 200 PG column (Pharmacia), which was pre-equilibrated with RB at 4 °C. The fraction corresponding to the histone octamer was collected, mixed with 50% (v/v) glycerol, and stored at −20 °C.

Assembly of Nucleosomes. The template for the nucleosome assembly was a 353 bp DNA fragment, containing stable sequence 601 (147 bp) for histone octamer binding (28) flanked by regions of 79 and 127 bp. The complete sequence of the DNA fragment is given as Supporting Information. The DNA was obtained by PCR amplification of plasmid pGEM3Z-601 with the following primers: 5'-CGG CCA GTG AAT TGT AAT ACG-3' and 5'-CGG GAT CCT AAT GAC CAA GG-3'. To reconstitute nucleosomes, the histone octamer was mixed with DNA in a 1:1 molar ratio in a buffer containing 10 mM Tris-HCl (pH 7.5) and 2 M NaCl and incubated for 30 min at room temperature. The mixture underwent a series of dilutions required by the protocol described in refs 26 and 27. The dialysis with three subsequent changes of the buffer, containing 10 mM Tris-HCl (pH 7.5) and 0.2 M NaCl, was performed at 4 °C with a 1 h incubation time at each step followed by overnight dialysis against the same buffer. The formation of NCP was controlled by the gel electrophoresis (5% PAGE) and AFM imaging in air.

AFM Imaging Methodology. The 1-(3-aminopropyl)silatrane (APS mica) (23, 29, 30) was used as a substrate for AFM imaging. The procedure for mica modification has been described previously (4). For experiments in air, NCPs in a buffer containing 10 mM Tris-HCl (pH 7.5) and 4 mM MgCl₂ were deposited on APS mica for 2 min, rinsed with deionized water (Aquamax Laboratory Water System, Aquamax Laboratory, Van Nuys, CA), and dried with argon gas. The images were collected on a NanoScope IIIId system (Veeco, Santa Barbara, CA) operating in tapping mode in air. Tapping mode etched silicon probes (TESP, Veeco) with a spring constant of 42 N/m and a resonant frequency between 270 and 320 kHz were used. The scan rate was 1.7 Hz. For experiments in liquid, the NCP sample in a buffer containing 10 mM Tris-HCl (pH 7.5) and 4 mM MgCl₂ was injected directly into the flow cell, avoiding the drying step. Images were acquired by using a NanoScope IIIId system operating in tapping mode in liquid using the protocols described previously (20–23). NP probes (NP, Veeco) with a spring constant of 0.06 N/m were used. The resonant peak at ca. 8 kHz was optimal for operation in aqueous solutions. Before the engagement, the initial parameters such as scan size and offset of the microscope were set to 0, and a piezo drive amplitude of ~100 mV (varied between 80 and 200 mV, corresponding to 2–7 nm of amplitude), a scan rate of ~1.5 Hz, and a set point

voltage of ~0.4 V were typically used. Typically, the drive amplitude was 2–3 times smaller than the initially selected value, but the values below 30 mV did yield stable images. The set point values were adjusted to the maximal stable values manually during scanning to maintain the high-resolution image and minimize the tip sweeping effect (20). The continued scanning over the selected area (~800 nm × ~800 nm image size) was performed to follow the dynamics of NCP, and images were recorded with a density of 512 × 512 points. Note that practically each deposited sample provided the images illustrating the high degree of reproducibility of the APS mica methodology (31, 32). Additional sample depositions in almost 100% of the cases were due to the need to replace the tip. Image processing for measuring the DNA contour length, arm lengths, the angle between DNA arms, and the protein volume was performed using Femtoscan (Advanced Technologies Center, Moscow, Russia) and is described in refs 30 and 33.

AFM Data Analysis. To estimate the number of DNA turns wrapped around the histone core from the length measurements, we used the following parameters for nucleosomes: 147 bp DNA is wrapped around the histones core making 1.7 turns (34, 35). The following equation for the dependence of the number of DNA turns around the histone core on arm length was used to calculate the number of turns for the NS:

$$\begin{aligned} \text{number of turns} &= 0.035L_{\text{wrapped around the core}} \\ &= 0.035[CL - (L_{\text{arm1}} + L_{\text{arm2}})] \end{aligned} \quad (1)$$

where CL is the contour length of free DNA and L_{arm1} and L_{arm2} are the lengths of short and long DNA arms, respectively. The angles between the arms were measured by drawing tangents to the section of the arms comprising 10 nm of the arm starting from the blob (30, 36).

RESULTS

The DNA template designed for this work was the fragment of 353 bp DNA containing 147 bp nucleosome positioning 601 sequence (7), flanked with two regions of different lengths, 79 and 127 bp. Such a design, similar to an early cryo-electron microscopy study (37), allowed us to map the nucleosome position and correlate it with the binding of the histone core to the central 147 bp region. Depending on the number of DNA turns around the histone core, the complex will adopt different morphologies schematically shown in Figure 1. The initial design corresponds to the complex with one turn, and four other schemes correspond to the complexes with 1.25, 1.5, 1.75, and 2 turns. All designs correspond to the uniform wrapping of both arms starting at the position in the center of the 147 bp region, so the lengths of the arms gradually decrease upon the DNA wrapping while the size






Nucleosome schematics					
Number of DNA turns	1	1.25	1.5	1.75	2
Rotation angle for long arm, deg	0	90	180	270	360
Length of wrapped DNA, bp	86	108	130	151	173

FIGURE 1: Schematics for nucleosome particles with different numbers of DNA supercoiling turns around the histone core.

of the nucleosome core is increasing. In addition, DNA wrapping is accompanied by a change in the interarm angle. We assign a value of zero to the rotation angle to the position of the long arm for the complex with one turn. The design with 1.25 DNA turns is characterized by a rotation angle of 90° . Therefore, the complexes with 1.5, 1.75, and 2 turns have rotation angles of 180° , 270° , and 360° , respectively. These parameters were used in the procedure of assigning the NCP structure.

The nucleosome sample prepared as described above was deposited onto APS mica, rinsed, dried, and imaged with AFM in air. Note that the sample was prepared without glutaraldehyde cross-linking. A typical AFM image of such samples is shown in Figure 2. The nucleosomes are clearly seen on these images as bright blobs with the DNA arms at both sides of the particle; however, the morphology of the particles is different. The yield of nucleosomal particles as shown in this image was ca. 60%. We marked the complexes with identical morphologies with the same numbers. The arms for particles marked as 1 are crossed. The arms are almost parallel for particles labeled as type 2, whereas the angle between the arms for particles labeled as type 3 is 180° . These images can be interpreted in terms of the different number of DNA turns around the histone core, and using the schematics in Figure 1, we assigned groups 1, 2, and 3 to particles with 1.75, 1.5, and 1 DNA turn, respectively. Note as well that blobs of NCP type 3 are less bright compared to those of types 1 and 2, suggesting that type 3 particles have the fewest DNA turns. AFM provides the height of the topographic images in addition to the lateral sizes, allowing one to calculate the volume values of the particles. The volume measurements were critical for analyses of

the protein stoichiometry of various specific protein–DNA complexes (30, 33). The dependence of the proteins' volume on their size obtained for proteins of different sizes is shown as a plot in Figure S0. The linearity of this plot justifies the use of the AFM volume values to estimate the protein molecular weight and was used for structural characterization of NCP. We interpret the variability of the particle size as an indication of NCP unwrapping, and on the basis of these data, we conclude that nucleosomes in solution are dynamic and capable of large-scale unwrapping. Thus, AFM imaging of non-cross-linked NCP samples in air revealed the structural heterogeneity of the particles, and we hypothesize that this heterogeneity reflects the inherent dynamics of NCP. To test this hypothesis and look directly at the dynamics of NCP in solution, we employed the AFM capability to perform imaging in aqueous solutions using time-lapse imaging of nondried NCP samples.

In time-lapse AFM mode, we performed continuous scanning over a selected area and followed the morphology changes of individual NCPs over time. The sample was deposited on APS mica and imaged without the drying step. The use of a functionalized APS mica surface allowed us to perform time-lapse experiments without restrictions to the composition of the buffer, and this methodology provided almost 100% reproducibility (21–23, 29). Several dozen time-lapse data sets were obtained and analyzed without any bias to the set. These experiments revealed different pathways, and the data below show the examples for each of these pathways. The imaging frames illustrating the dynamics of one selected NCP particle are shown in figures, and sets of frames arranged as movie files for each data set appear as Supporting Information.

Figure 3 shows the images and the data for a pathway characterized by two-step changes of the NCP. The frame-by-frame images are shown in Figure 3A, and the set of images assembled as a movie appears as Supporting Information (M1 file). Initially, the NCP with short arms of DNA slightly changes its conformation (frames 1 and 2) and then unwraps in frame 3. The NCP retains its geometry over three frames in a row (frames 3–5). Then, between frames 5 and 6, it loosens, unwraps, again in frame 6, stays unchanged in frame 7, and finally undergoes full dissociation in frame 8. This data set shows also that the NCP dynamics is accompanied by elongation of both DNA arms and a decrease in the size of the blob as well a change in the interarm angle. As we mentioned above (see Materials and Methods), these parameters were used for the characterization of the NCP geometry in each frame.

The values of arm length, depending on the frame number, are plotted in Figure 3B. The graphs show that, over time, arms increase in length. The arm lengths were used for calculation of the number of DNA turns within the nucleosome for each frame, and the data are shown in Figure 3C (triangles, black line). This

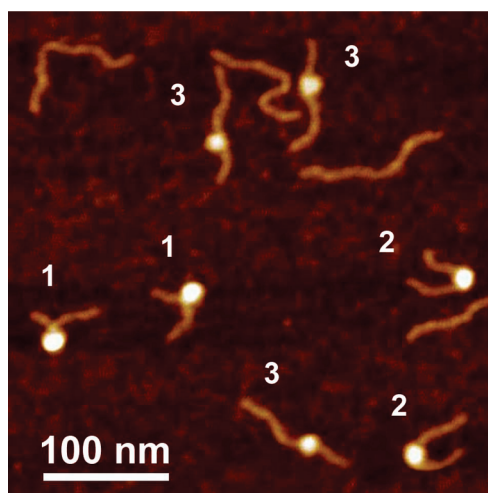


FIGURE 2: AFM image taken in air of the nucleosome samples. Nucleosomes marked with numbers 1.7, 1.4, and 1.0 correspond to NCPs with ~ 1.7 , ~ 1.4 , and ~ 1.0 turn of DNA wrapped around the core particle, respectively.

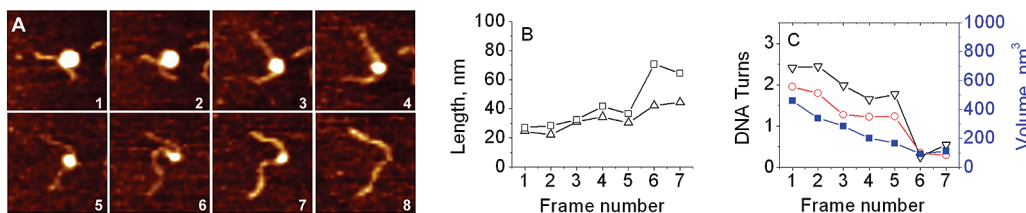


FIGURE 3: Two-step unwrapping process. (A) Consecutive AFM images of nucleosomes with the two-step unwrapping process, taken during continuous scanning in the buffer. Each frame is 200 nm. (B) Dependence of arm length on frame number. (C) Dependence of the number of DNA turns around the core calculated from arm lengths (black) and from angles between DNA arms (red) on frame number. The dependence of nucleosome volume on frame number is shown in blue (right Y-axis). Each frame takes ~ 170 s to scan.

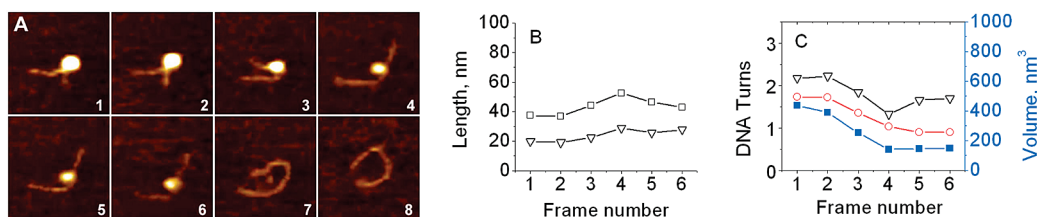


FIGURE 4: One-step unwrapping process. (A) Consecutive AFM images of nucleosomes with one-step unwrapping, taken during continuous scanning in the buffer. The scan size is 100 nm. (B) Dependence of arm length (in nanometers) on frame number. (C) Dependence of the number of DNA turns around the core calculated from arm lengths (black) and from angles between DNA arms (red) on frame number. The dependence of nucleosome volume on frame number is shown in blue (right Y-axis). Each frame takes ~ 170 s to scan.

NCP particle initially has ~ 2.5 turns (frame 1), remains unchanged in frame 2, releases ~ 0.75 turn in frames 3 and 4, stays with 1.75 turns between frames 4 and 5, and then unwraps for 1.2 turns between frames 5 and 6, followed by histone core dissociation in frame 8. The number of turns was also determined using the measurements of the interarm angles, and the data are shown with circles (red line) in Figure 3C. This time dependence of the DNA turns is qualitatively very similar to the previous one, although the values of the DNA turns measured by this method are slightly different. We consider such a pattern of nucleosome dynamics as a two-step unwrapping process. The DNA wrapping of the histone cores contributes to the overall volume of the NCP particle, so we measured the volumes of NCP on each frame and plotted these values in Figure 3C (blue squares). This plot shows that the NCP volumes decrease over time (the number of the frame), supporting the idea to use this parameter for the NCP characterization. The dependence is rather smooth and does not exhibit plateaus revealed by the two previous methods, indicating the limited accuracy of the volume measurements for estimation of the number of DNA turns in the NCP particle.

Figure 4 illustrates another type of NCP dynamics, one-step gradual unfolding. Similar to the previous data set, frames of the images are shown in Figure 4A, and an animated set appears as Supporting Information (M2 file). The quantitative analysis of this pathway is presented in panels B and C of Figure 4. According to the arm length measurements (black triangles), the NCP initially with 2.25 turns is stable for two frames, then loses ~ 1 turn between frames 2 and 4, and stays with 1.5 turns for three more frames until finally the histone core dissociates (frame 7). Again, the NCP dynamics revealed by the angle measurements (red circles) shows a similar pattern. The volume change (blue solid squares) follows the pattern of the DNA unwrapping curves.

Panels A and B of Figure 5 show the results of the analysis of additional sets of the data for one-step and two-step unfolding processes, illustrating the dynamics of rather stable NCP particles. The images and the data for the arm lengths are shown as Figures S1 and S2, respectively, along with the corresponding movie files M3 and M4 in the Supporting Information. The one-step unfolding process of the NCP with ~ 2 DNA turns (Figure 5A and movie M3) starts rather late, so the particle remains stable during four consecutive scanning frames (frames 1–4). The unwrapping occurs between frames 4 and 6 with 1 DNA turn left followed by a complete unwrapping of the DNA and dissociation of the histone core detected after frame 7.

Figure 5B shows the data for a rather interesting two-step dissociation pattern (see the images in Figure S2A,B and movie M4 in the Supporting Information). This NCP, after an initial rapid loss of ~ 0.75 DNA turn (frame 2), remains stable (seven frames), although the arms move around the core in a rather

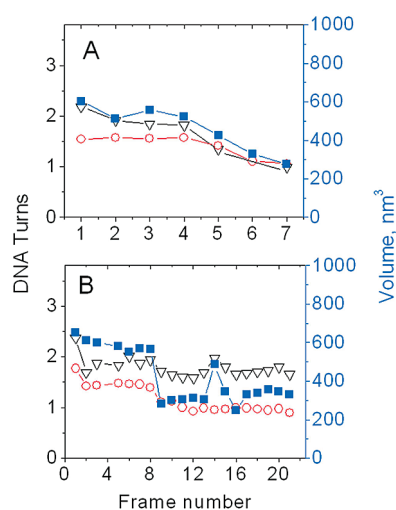


FIGURE 5: Dependence of the number of DNA turns around the core calculated from arm lengths (black) and from angles between the DNA arms (red) on frame number for two sets of the data shown in Figures S1 and S2, respectively. The dependence of nucleosome volume on frame number is shown in blue (right Y-axis).

broad range. Between frames 8 and 9, this NCP loses 0.25 turn and remains very stable for another 13 frames. Final dissociation of the histone core is seen in frame 22. Note the increase in the number of DNA turns (~ 0.25 turn) between frames 12 and 14 followed by the decrease in the number of turns by the same value. This dynamics of NCP is detected by the volume measurements (filled squares).

DISCUSSION

The experiments described above show directly that NCP particles are so dynamic that large DNA segments are capable of unwrapping from the NCP core. This process can lead to full dissociation of nucleosomes. In addition, these data provide insight into the mechanism of nucleosome dynamics.

Generally, two models are considered for NCP dynamics. According to the site exposure model, DNA spontaneously dissociates from the core histones via unwrapping from the ends of the nucleosome, and the results of the fluorescence studies, including single-molecule analysis (8, 10, 11), favor the site exposure model. Moreover, it was shown that unwrapping of DNA is an intrinsic property of NCP, and under physiological conditions, individual NCPs are partially unwrapped ~ 2 –10% of the time (2). The alternative model, known as the sliding model, where the core moves along the template was observed mainly in the presence of chaperones or modified histones (e.g., refs 38 and 39).

Single-molecule time-lapse AFM data allowed us to distinguish between the two models. Indeed, as the histone core slides

and/or rolls, one of the arms becomes longer and another arm becomes shorter. Other structural parameters of NCPs, such as the size of the nucleosome and the angle between the arms, should remain unchanged over time. The expectations for the NCP structure of the site exposure model are different. First, the dissociation step is accompanied by the elongation of both arms of the NCP. Second, because of the removal of the DNA from the NCP core, the nucleosome particles decrease in size. Third, the angle between the arms should vary as well. Our data, regardless of the particular DNA dissociation pathway, reveal the same pattern: both arms of the NCP become longer; this process is accompanied by a decrease in the nucleosome size and a change in the interarm angles. Therefore, the AFM data are in line with the site exposure model. Interestingly, this model is also supported by the imaging in air of dry NCP samples. As shown in Figure 2, there is no same size NCP with different arm lengths that should appear if cores are able to slide along the DNA fragment. Only the two opposite parameters, the blob sizes and interarm angles, are varied. We cannot exclude the possibility that the DNA sequence contributes to this particular NCP dynamics pathways as the stability of NCP is DNA sequence-dependent (1, 2, 10, 40–42), so the sequences other than the 601 type will follow the sliding model. However, for the 601 DNA sequence selected for this study, the sliding pattern has not been observed.

There is a common feature for various pathways of NCP dissociation: the particles with ~ 1 DNA turn are rather unstable, so the nucleosome should wrap more DNA or should dissociate. The time-lapse data also provide information about the core structure at the very last stage of the NCP unwrapping process. Figure 3A (the two-step process) shows that a small blob remains on the full-length DNA substrate (frames 6 and 7), disappearing in the last frame. Similar complexes with small blobs can be seen in Figure 4A (frames 5 and 6). These are histone cores that remain bound to the DNA template, so we are able to estimate the stoichiometry of the cores on the basis of the molecular weight values obtained from the volume measurements (30, 33). This analysis shows that the anticipated volume of the histone octamer (108 kDa) should be in the range of 210 nm^3 . The size of the blob in Figure 3C (frames 6 and 7) is smaller than this anticipated value. Interestingly, the volumes of blobs for frames 4–6 of Figure 4C (one-step process) are also smaller than 200 nm^3 , although ~ 1 DNA turn remains on this particle. These observations suggest that in some NCP complexes, the histone core undergoes partial dissociation prior to the complete DNA unwrapping. At the same time, the volume data in panels A and B of Figure 5 are of a different type: the sizes of blobs prior to the dissociation are larger than 200 nm^3 , suggesting that no histone dissociation took place. Another example of the dissociation of the full core is shown in the Supporting Information (Figure S3, one-step full dissociation, and movie file M5), and data analyses of arm lengths, protein volumes, and numbers of turns are shown in panels B and C of Figure S3, respectively. Thus, these data suggest that when the DNA unwraps, different pathways with and without partial dissociation of the histones exist and the selection of the pathway may depend on the local environment around each particular NCP. There is biochemical evidence indicating that H2A–H2B dimers can be depleted (see review 43 and also refs 2 and 16), and this process facilitates the next DNA unwrapping step. The role of H2A–H2B histones in NCP stability and dynamics has been revealed in the recent single-molecule FRET experiments (44, 45), and this important issue has been discussed recently (42).

Thus, the time-lapse AFM data present a picture of the NCP complexes as very dynamic biomolecular systems, in which large DNA segments are capable of dissociating from the NCP particle. Our hypothesis is that the observed unwrapping is due to the thermal motion of nucleosomes rather than the AFM tip sweeping effect. There are a number of major pieces of evidence supporting this assumption. First, AFM images of dried samples show a wide heterogeneity of nucleosome morphologies, and essentially the same heterogeneity has been observed in the time-lapse single-molecule imaging experiments. Second, for the same sample, the unwrapping rate for nucleosomes varies over a broad range. It can be relatively fast, so a complete unwrapping occurs over a few frames (six frames in Figures 3 and 4) or relatively slow with very subtle changes in DNA arms lengths (Figure 5B, frames 1–8). Note that the scanning conditions in these experiments were identical and the same AFM tip was used. Third, we performed experiments in which the scanned and unscanned areas were compared. In these experiments, the large area was scanned once, then a smaller area was selected, and continuous scanning over this area was performed until essentially all nucleosomes in the area dissociated. The microscope was unzoomed to the original large area that was rescanned. If the nucleosome unwrapping were caused by the scanning tip only, we would observe NCP unwrapping over the small area with little or no change in the nucleosome morphology in the rest of the image. The data for one of these experiments are shown in Figure S5; these images show that unwrapped nucleosomes were observed in both areas. Thus, the observed dissociation of nucleosomes is not due to the tip sweeping effect. However, we cannot exclude some “pushing” effect of the AFM tips facilitating unwrapping, as a few nucleosomes on the unscanned area remain compared to only one (right edge) on the scanned area.

The dynamics of nucleosomes on the 50–100 ms time scale corresponds to the fluctuation of the DNA arms at the very edge of the particle (8). Our AFM experiments revealed unwrapping of much larger DNA segments, including full unwrapping of nucleosomes. Note the recent publications in which large-scale dynamics of NCP was detected with single-molecule FRET (46, 47). Additional indirect evidence of the large-scale dynamics of nucleosomes comes from the recent paper (9) in which the dynamics of nucleosomes *in vivo* was probed by the DNA repair with photolyase. These data also revealed the dynamics of nucleosomes at the particle edges on a second time scale, but all lesions within the nucleosome were repaired in 2 h, suggesting that accessibility of internal regions is limited, and long times are required for exposing remote regions within nucleosomes. If large-scale unwrapping was required for the internal probing of nucleosomes, the obtained data suggest that the time scale for such a process is much larger than the time scale of seconds for the small-range fluctuations. It was proposed recently (8) that large-range dynamics of nucleosomes may employ a stepwise unwrapping process in which initial unwrapping starts at the edge of the nucleosomal DNA and moves inward. Therefore, the movement of the unwrapped segment inside the nucleosome is a multistep process in which unwrapping of large regions requires long times.

It is tempting to extract the characteristic times from the single-molecule AFM data, but these values cannot be obtained for two major reasons. First, the temporal resolution of the traditional AFM instrument does not allow us to acquire the data with a rate faster than one frame per minute. According to the data of Li et al. (8), unwrapping occurs on the millisecond time scale.

Therefore, special AFM techniques with considerably higher temporal resolution are needed. Note, however, in some of the time trajectories for the arms lengths [Figures S2B and S4B (set of data in Figure S4 and movie file M6)], we observed wrapping/unwrapping events suggesting that the use of an instrument with a higher temporal resolution may enable us to visualize more details of the NCP dynamics paths. Second, AFM is a topographic technique requiring the sample to be bound to the surface. We used a positively charged APS mica surface that has an elevated affinity for negatively charged DNA filaments compared to NCP particles. However, the APS mica protocol permits us to control the strength of the sample–surface interaction, allowing us to observe DNA dynamics at the surface–liquid interface. At the same time, the interaction of the NCP samples with the surface is the factor that may change the NCP dynamics. We hypothesize that transiently unwrapped DNA segments can be trapped by electrostatic interactions with the surface, increasing the probability of the next unwrapping step. These interactions shift the equilibrium of the unwrapping/wrapping dynamics toward unwrapping that eventually leads to full unwrapping of the nucleosome.

The hypothesis about the effect of electrostatic interactions on the NCP dynamics prompts new ideas about potential mechanisms for the regulation of unwrapping of NCP within chromatin. Large remodeling systems are involved in the regulation of chromatin dynamics; however, the mechanism by which they perform nucleosome unwrapping is unclear. For example, in the wave–ratchet–wave model for ISWI remodeler, a small internal loop is moved along the DNA within the nucleosome (3). The requirement for a small loop was proposed to meet the energy needs for the unwrapping process. However, the necessary energy deficit can be provided by electrostatics. If electrostatic interactions of free DNA with a positively charged surface increase the NCP dynamics, the DNA–surface contacts provided by positively charged groups located on the surfaces of the remodeling proteins facing the chromatin surface will shift the fluctuation toward the unwrapping step. Our early estimates of surface charge density of similar aminopropyl mica provided quite low values for the positive charge density, ca. one unit per an area of several nanometers (20), suggesting that a quite limited number of nonspecific electrostatic in nature contacts may shift the equilibrium toward unwrapping. In addition to remodeling protein complexes, positive charges for the contacts with chromatin can be provided by intranuclear surfaces. Therefore, we speculate that the interaction of chromatin with these surfaces can provide an additional contribution to the chromatin dynamics facilitating unwrapping of the chromatin. Therefore, APS mica can be considered as a model system for understanding the role of electrostatic interactions between the chromatin and intracellular membranes in the regulation of chromatin dynamics and gene activity.

ACKNOWLEDGMENT

We thank I. Nazarov for the help in the preparation of nucleosome samples, J. Widom and C. Woodcock for critical reading of the manuscript and useful comments, and Alex Portillo for proofreading the manuscript.

SUPPORTING INFORMATION AVAILABLE

Full sequence of the DNA fragment studied in this paper, dependence of the protein volume measured with AFM on

protein molecular weight, images and graphs for different modes of NCP dynamics (full dissociation, wrapping/unwrapping, and one-step full dissociation), large-scale AFM images in aqueous solution, and movie files for animated data sets of time-lapse images. This material is available free of charge via the Internet at <http://pubs.acs.org>.

REFERENCES

1. Luger, K., and Hansen, J. C. (2005) Nucleosome and chromatin fiber dynamics. *Curr. Opin. Struct. Biol.* 15, 188–196.
2. Thoma, F. (2005) Repair of UV lesions in nucleosomes: Intrinsic properties and remodeling. *DNA Repair* 4, 855–869.
3. Saha, A., Wittmeyer, J., and Cairns, B. R. (2006) Chromatin remodeling: The industrial revolution of DNA around histones. *Nat. Rev. Mol. Cell Biol.* 7, 437–447.
4. Cairns, B. R. (2007) Chromatin remodeling: Insights and intrigue from single-molecule studies. *Nat. Struct. Mol. Biol.* 14, 989–996.
5. Ahmad, K., and Henikoff, S. (2002) Epigenetic consequences of nucleosome dynamics. *Cell* 111, 281–284.
6. Anderson, J. D., Thastrom, A., and Widom, J. (2002) Spontaneous access of proteins to buried nucleosomal DNA target sites occurs via a mechanism that is distinct from nucleosome translocation. *Mol. Cell Biol.* 22, 7147–7157.
7. Li, G., and Widom, J. (2004) Nucleosomes facilitate their own invasion. *Nat. Struct. Mol. Biol.* 11, 763–769.
8. Li, G., Levitus, M., Bustamante, C., and Widom, J. (2005) Rapid spontaneous accessibility of nucleosomal DNA. *Nat. Struct. Mol. Biol.* 12, 46–53.
9. Bucci, A., Kapitzka, K., and Thoma, F. (2006) Rapid accessibility of nucleosomal DNA in yeast on a second time scale. *EMBO J.* 25, 3123–3132.
10. Tims, H. S., and Widom, J. (2007) Stopped-flow fluorescence resonance energy transfer for analysis of nucleosome dynamics. *Methods* 41, 296–303.
11. Koopmans, W. J., Brehm, A., Logie, C., Schmidt, T., and van Noort, J. (2007) Single-pair FRET microscopy reveals mononucleosome dynamics. *J. Fluoresc.* 17, 785–795.
12. Leuba, S. H., Yang, G., Robert, C., Samori, B., van Holde, K., Zlatanova, J., and Bustamante, C. (1994) Three-dimensional structure of extended chromatin fibers as revealed by tapping-mode scanning force microscopy. *Proc. Natl. Acad. Sci. U.S.A.* 91, 11621–11625.
13. Leuba, S. H., Bustamante, C., Zlatanova, J., and van Holde, K. (1998) Contributions of linker histones and histone H3 to chromatin structure: Scanning force microscopy studies on trypsinized fibers. *Biophys. J.* 74, 2823–2829.
14. Yodh, J. G., Lyubchenko, Y. L., Shlyakhtenko, L. S., Woodbury, N., and Lohr, D. (1999) Evidence for nonrandom behavior in 208-12 subsaturated nucleosomal array populations analyzed by AFM. *Biochemistry* 38, 15756–15763.
15. Yodh, J. G., Woodbury, N., Shlyakhtenko, L. S., Lyubchenko, Y. L., and Lohr, D. (2002) Mapping nucleosome locations on the 208-12 by AFM provides clear evidence for cooperativity in array occupation. *Biochemistry* 41, 3565–3574.
16. Nikova, D. N., Pope, L. H., Bennink, M. L., van Leijenhorst-Groener, K. A., van der Werf, K., and Greve, J. (2004) Unexpected binding motifs for subnucleosomal particles revealed by atomic force microscopy. *Biophys. J.* 87, 4135–4145.
17. Guthold, M., Bezanilla, M., Erie, D. A., Jenkins, B., Hansma, H. G., and Bustamante, C. (1994) Following the assembly of RNA polymerase-DNA complexes in aqueous solutions with the scanning force microscope. *Proc. Natl. Acad. Sci. U.S.A.* 91, 12927–12931.
18. Hansma, H. G., Bezanilla, M., Zenhausern, F., Adrian, M., and Sinsheimer, R. L. (1993) Atomic force microscopy of DNA in aqueous solutions. *Nucleic Acids Res.* 21, 505–512.
19. Bustamante, C., Rivetti, C., and Keller, D. J. (1997) Scanning force microscopy under aqueous solutions. *Curr. Opin. Struct. Biol.* 7, 709–716.
20. Lyubchenko, Y. L., and Shlyakhtenko, L. S. (1997) Visualization of supercoiled DNA with atomic force microscopy in situ. *Proc. Natl. Acad. Sci. U.S.A.* 94, 496–501.
21. Mikheikin, A. L., Lushnikov, A. Y., and Lyubchenko, Y. L. (2006) Effect of DNA supercoiling on the geometry of holliday junctions. *Biochemistry* 45, 12998–13006.
22. Lushnikov, A. Y., Bogdanov, A., and Lyubchenko, Y. L. (2003) DNA recombination: Holliday junctions, dynamics and branch migration. *J. Biol. Chem.* 278, 43130–43134.

23. Lyubchenko, Y. L. (2004) DNA structure and dynamics: An atomic force microscopy study. *Cell Biochem. Biophys.* 41, 75–98.
24. Ando, T., Uchihashi, T., Koder, N., Yamamoto, D., Taniguchi, M., Miyagi, A., and Yamashita, H. (2007) High-speed atomic force microscopy for observing dynamic biomolecular processes. *J. Mol. Recognit.* 20, 448–458.
25. Crampton, N., Roes, S., Dryden, D. T., Rao, D. N., Edwardson, J. M., and Henderson, R. M. (2007) DNA looping and translocation provide an optimal cleavage mechanism for the type III restriction enzymes. *EMBO J.* 26, 3815–3825.
26. Luger, K., Rechsteiner, T. J., and Richmond, T. J. (1999) Preparation of nucleosome core particle from recombinant histones. *Methods Enzymol.* 304, 3–19.
27. Dyer, P. N., Edayathumangalam, R. S., White, C. L., Bao, Y., Chakravarthy, S., Muthurajan, U. M., and Luger, K. (2004) Reconstitution of nucleosome core particles from recombinant histones and DNA. *Methods Enzymol.* 375, 23–44.
28. Lowary, P. T., and Widom, J. (1998) New DNA sequence rules for high affinity binding to histone octamer and sequence-directed nucleosome positioning. *J. Mol. Biol.* 276, 19–42.
29. Shlyakhtenko, L. S., Gall, A. A., Filonov, A., Cerovac, Z., Lushnikov, A., and Lyubchenko, Y. L. (2003) Silatrane-based surface chemistry for immobilization of DNA, protein-DNA complexes and other biological materials. *Ultramicroscopy* 97, 279–287.
30. Lushnikov, A. Y., Potaman, V. N., Oussatcheva, E. A., Sinden, R. R., and Lyubchenko, Y. L. (2006) DNA strand arrangement within the SfiI-DNA complex: Atomic force microscopy analysis. *Biochemistry* 45, 152–158.
31. Lyubchenko, Y. L., and Shlyakhtenko, L. S. (2009) AFM for analysis of structure and dynamics of DNA and protein-DNA complexes. *Methods* 47, 206–213.
32. Lyubchenko, Y. L., Shlyakhtenko, L. S., and Gall, A. A. (2009) Atomic force microscopy imaging and probing of DNA, proteins, and protein DNA complexes: Silatrane surface chemistry. *Methods Mol. Biol.* 543, 337–351.
33. Shlyakhtenko, L. S., Gilmore, J., Portillo, A., Tamulaitis, G., Siksnys, V., and Lyubchenko, Y. L. (2007) Direct visualization of the EcoRII-DNA triple synaptic complex by atomic force microscopy. *Biochemistry* 46, 11128–11136.
34. Luger, K., Mader, A. W., Richmond, R. K., Sargent, D. F., and Richmond, T. J. (1997) Crystal structure of the nucleosome core particle at 2.8 Å resolution. *Nature* 389, 251–260.
35. Feng, J., and Chun-Cheng, Z. (2007) Thermodynamics of nucleosomal core particles. *Biochemistry* 46, 2594–2598.
36. Pavlicek, J. W., Oussatcheva, E. A., Sinden, R. R., Potaman, V. N., Sankey, O. F., and Lyubchenko, Y. L. (2004) Supercoiling-induced DNA bending. *Biochemistry* 43, 10664–10668.
37. Furrer, P., Bednar, J., Dubochet, J., Hamiche, A., and Prunell, A. (1995) DNA at the entry-exit of the nucleosome observed by cryoelectron microscopy. *J. Struct. Biol.* 114, 177–183.
38. Chakravarthy, S., Park, Y. J., Chodaparambil, J., Edayathumangalam, R. S., and Luger, K. (2005) Structure and dynamic properties of nucleosome core particles. *FEBS Lett.* 579, 895–898.
39. Park, Y. J., Chodaparambil, J. V., Bao, Y., McBryant, S. J., and Luger, K. (2005) Nucleosome assembly protein 1 exchanges histone H2A-H2B dimers and assists nucleosome sliding. *J. Biol. Chem.* 280, 1817–1825.
40. Luger, K. (2006) Dynamic nucleosomes. *Chromosome Res.* 14, 5–16.
41. van Holde, K., and Zlatanova, J. (2006) Scanning chromatin: A new paradigm? *J. Biol. Chem.* 281, 12197–12200.
42. Sharma, S., and Dokholyan, N. V. (2008) DNA sequence mediates nucleosome structure and stability. *Biophys. J.* 94, 1–3.
43. Kimura, H. (2005) Histone dynamics in living cells revealed by photobleaching. *DNA Repair* 4, 939–950.
44. Kelbauskas, L., Chan, N., Bash, R., Yodh, J., Woodbury, N., and Lohr, D. (2007) Sequence-dependent nucleosome structure and stability variations detected by Förster resonance energy transfer. *Biochemistry* 46, 2239–2248.
45. Kelbauskas, L., Chan, N., Bash, R., DeBartolo, P., Sun, J., Woodbury, N., and Lohr, D. (2008) Sequence-dependent variations associated with H2A/H2B depletion of nucleosomes. *Biophys. J.* 94, 147–158.
46. Tomschik, M., van Holde, K., and Zlatanova, J. (2009) Nucleosome dynamics as studied by single-pair fluorescence resonance energy transfer: A reevaluation. *J. Fluoresc.* 19, 53–62.
47. Tomschik, M., Zheng, H., van Holde, K., Zlatanova, J., and Leuba, S. H. (2005) Fast, long-range, reversible conformational fluctuations in nucleosomes revealed by single-pair fluorescence resonance energy transfer. *Proc. Natl. Acad. Sci. U.S.A.* 102, 3278–3283.